ACCURATE NONLINEAR MODELING AND VERIFICATION OF MMIC AMPLIFIER

Vincent D. Hwang, Yi-Chi Shih, and Huy M. Le

Hughes Aircraft Company
Microwave Products Division
Torrance, California 90509-2940

ABSTRACT

An accurate MESFET nonlinear model and a reliable model verification approach which uses the on-wafer RF probing method are presented. The nonlinear model is based on small signal S-parameter characterization of the MESFET at a wide range of bias voltages. Simulation results of an MMIC amplifier at various frequencies, bias voltages, and power levels agree well with the measurement data.

INTRODUCTION

An accurate nonlinear MESFET model and a reliable model verification approach are presented. The nonlinear model is developed from S-parameter measurements of a MESFET at various bias voltages. As shown in this work, this "RF" curve-fitted model is capable of accurately predicting the MMIC amplifier performances at various bias voltages, frequencies, and input power levels (both small and large signals).

A novel model verification scheme is designed to eliminate many measurement uncertainties. In this approach, the nonlinear model is verified by comparing the simulation results of a single-stage MMIC amplifier with the measurement data. The S-parameters of the amplifier's input and output matching circuits are first accurately measured using the on-wafer RF probes. These data are then input to the simulation program for the complete amplifier simulation. In this way, the uncertainties of the matching circuits' impedances and loss are eliminated, and the MESFET model can be verified with a high degree of confidence by comparing the amplifier simulation and the measurement data.

The nonlinear model accurately predicts the MMIC amplifier's frequency response at various input power levels, and the amplifier's power saturation curves.

NONLINEAR MESFET MODELING

Many nonlinear MESFET models (1-3) are based on curve-fitting of the device's channel current expression to the measured dc I-V curves. These dc fitted models ignore the fact that MESFET's transconductance and output resistance are frequency dispersive at low frequency range (below 100 MHz) (4,5). Because the dc G_m and R_o values are higher than the RF ones, the dc fitted models tend to predict higher gain and output power.

In this work, the MESFET model is developed from S-parameter measurements at various bias voltages. Since this model is fitted to the high frequency RF data, the low frequency dispersion characteristics of G_m and R_o do not affect the model's accuracy in predicting the device's RF performances. This "RF" fitted model is developed by the following steps:

1. Measure the MESFET's S-parameters at a wide range of bias voltages using on-wafer RF probes.

2. Fits the MESFET small signal equivalent circuit to the S-parameter measured in Step 1.

3. The MESFET's nonlinear elements versus bias voltages curves are plotted out. Figures 1 through 3 are the G_m, R_o, and C_{gs} curves.

4. Empirical expressions of $I_{ch}(V_g,V_d)$, and $C_{gs}(V_g,V_d)$ of the large signal equivalent circuit (Figure 4) are fitted to the curves of Figures 1 through 3. The expression for C_{gs} is

$$C_{gs}(V_g, V_d) = [C_o/(1 - V_g/V_b)^r](1 + bV_d) + d \qquad (1)$$

where C_o, V_b, r, b, and d are the fitting parameters. The expression for $I_{ch}((V_g,V_d)$ is

$$I_{ch}(V_g, V_d) = X_5(V_g + X_2)^{1.5}\tanh(X_1V_d) - (X_3 + X_4V_g)^2V_d + \frac{V_d}{(X_6 + X_7V_d)} \qquad (2)$$

where X_1 through X_7 are the fitting parameters. These fitting parameters are optimized so that the partial derivatives of I_{ch}, $\partial I_{ch}/\partial V_g$ and $\partial I_{ch}/\partial V_d$ are fitted to the G_m and R_o curves.

5. The breakdown current, I_{br}, and the gate forward current, I_g, are fitted to the pulse measured gate current versus gate and drain voltages data. The expression for I_{br} is

$$I_{br}(V_g, V_d) = I_o * \exp(r_1 * V_d - r_2 * V_g) \qquad (3)$$

where I_o, r_1, and r_2 are the fitting parameters.

89CH2761-5/89/0000-0037$01.00 © 1988 IEEE

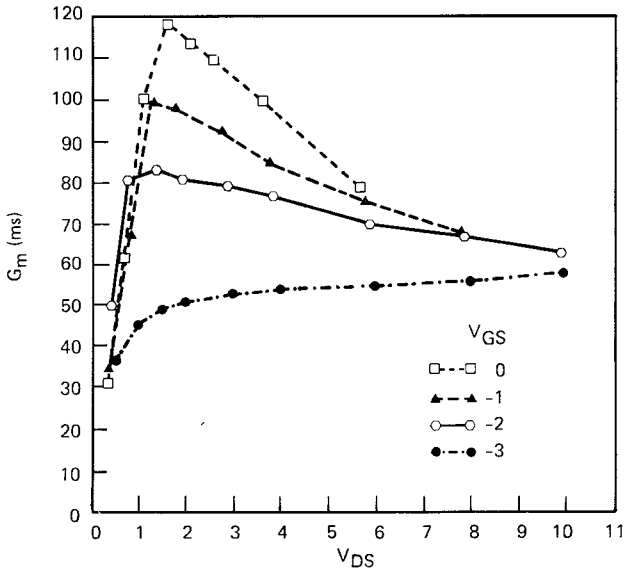

Figure 1 G_m versus V_{GS} and V_{DS} curves.

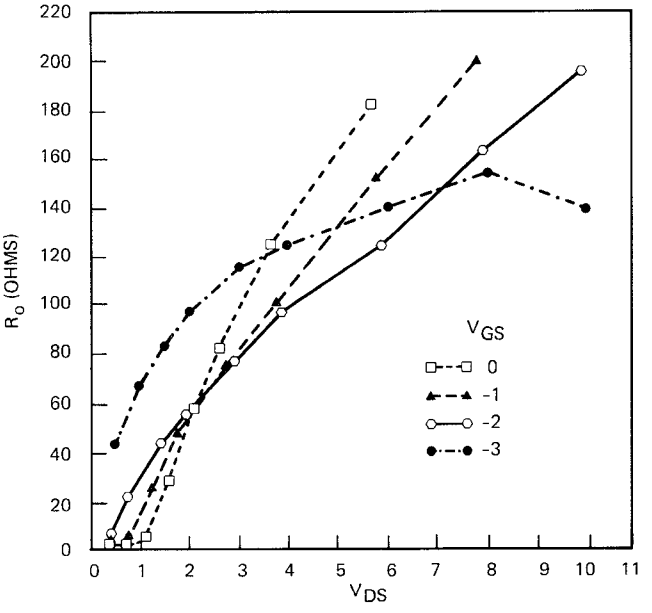

Figure 2 R_o versus V_{GS} and V_{DS} curves.

The nonlinear model is simulated by a nonlinear circuit analysis computer program developed in-house which is based on the algorithm proposed in the work of P.W. Van Der Walt (6).

MODEL VERIFICATION

In the past, MESFET nonlinear models are often verified by measuring the power performances of a MESFET device mounted on a test fixture. In the conventional approach, reliable measurement data are difficult to obtain due to uncertainties in determining the tuners and fixture loss, and the impedances presented to the MESFET. In our verification approach, the S-parameters of the input and output matching circuits of a MMIC amplifier are directly measured by on-wafer

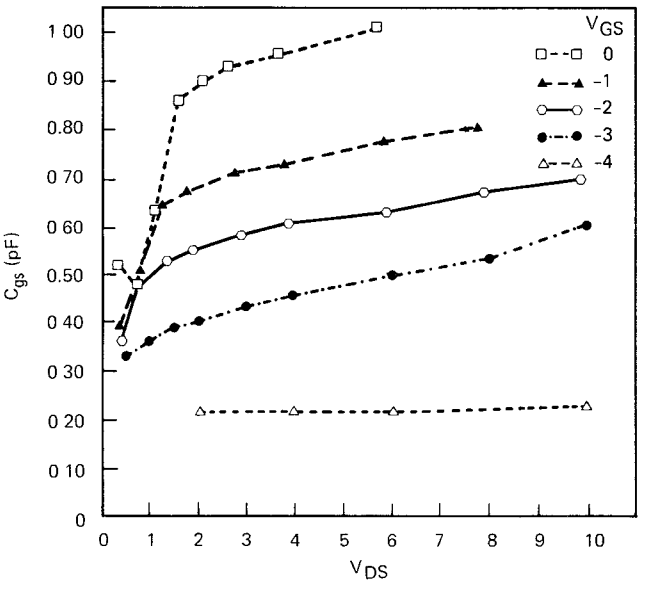

Figure 3 C_{gs} versus V_{GS} and V_{DS} curves.

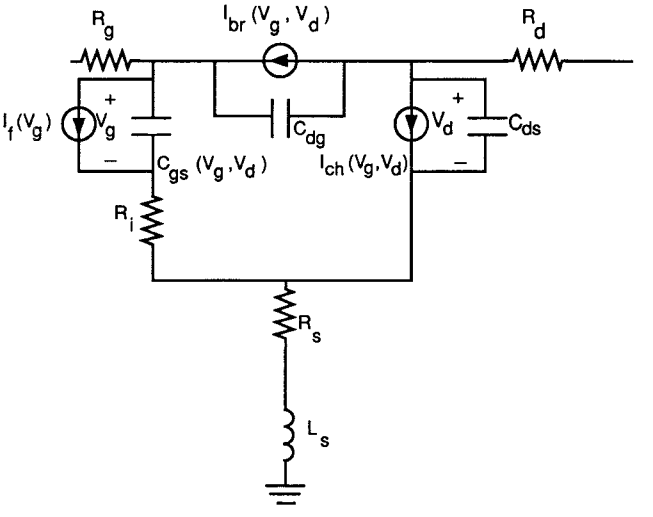

Figure 4 MESFET large-signal equivalent circuit.

probes. Using these S-parameters in the amplifier simulation, the computer program can accurately determine the impedances presented to the MESFET and the losses in the matching circuits.

To verify the nonlinear model, a single-stage MMIC amplifier, its matching circuit dropouts, and the MESFET device dropouts are fabricated on the same wafer. Figure 5 presents the photographs of the amplifier, the matching circuits, and the MESFET dropouts. The MESFET nonlinear model is developed by on-wafer characterizing the MESFET dropout. Since the MESFET is fabricated on the same wafer with the amplifier, the uncertainty due to the process variation is reduced when the measurement and simulation data are compared later. To simulate the amplifier, the S-parameters of the input and output matching circuits need to be known. These S-parameters are accurately measured by on-wafer

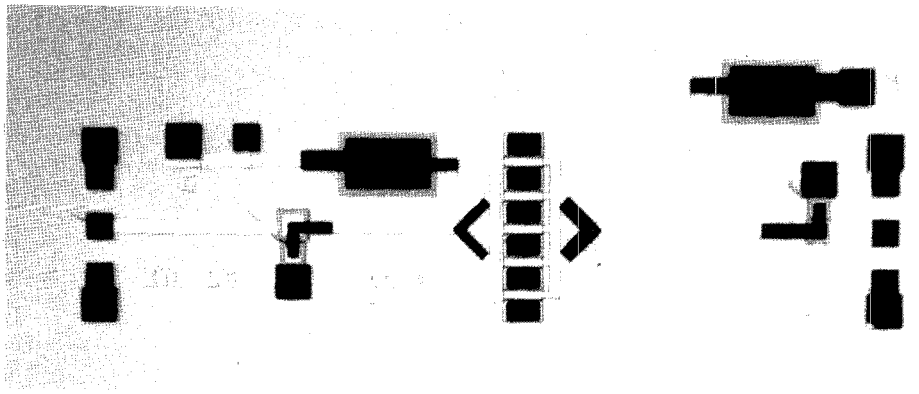

MMIC SINGLE STAGE AMPLIFIER

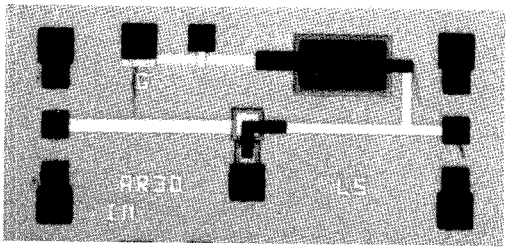

INPUT MATCHING CIRCUIT

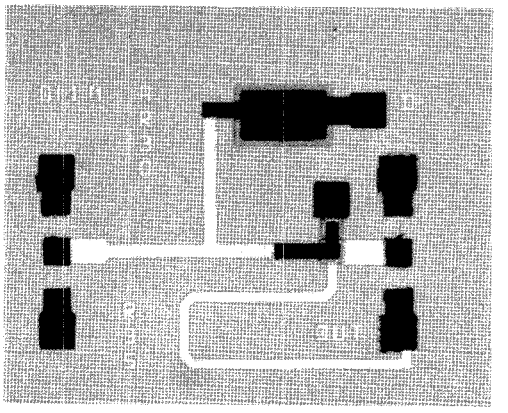

OUTPUT MATCHING CIRCUIT

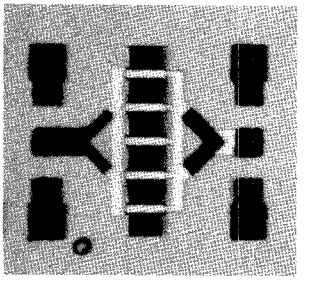

MESFET DROP-OUT

Figure 5 Photographs of the MMIC amplifiers and its drop-outs.

probing the matching circuit dropouts. The amplifier circuit is first on-wafer characterized for its small signal gain. It is then diced and mounted on a test fixture for power testing.

RESULTS

Figures 6 and 7 show the simulated and measured amplifier P_{out} versus P_{in} curves at 10.65 GHz for three different bias voltages. It can be seen that the model accurately predicts the saturation characteristics at different bias voltages. Figures 8 and 9 show the simulated and measured curves of P_{out} versus frequency at different input power levels. As shown, the agreement between the simulation and measurement data are excellent across the frequency band and different input power levels.

CONCLUSION

An accurate MESFET large signal model is presented. The model is validated by a verification scheme that eliminates many measurement uncertainties.

REFERENCES

(1) Y. Tajima, *et al.*, "GaAs FET large signal model and its application to circuit design," *IEEE Trans. Elec. Devices*, Vol. ED-28, pp. 171-175, Feb. 1981.

(2) A. Materka, *et al.*, "Computer calculation of large signal GaAs FET amplifier characteristics," *IEEE Trans. Microwave Theory Tech.*, Vol. MTT-33, pp. 129-134, Feb. 1985.

(3) W. Curtice and M. Ettenger, "A nonlinear GaAs FET model for use in the design of output circuit for power amplifiers," *IEEE Trans. Microwave Theory Tech.*, Vol. MTT-33, pp. 1383-1393, Dec. 1985.

(4) P. Canfield, J. Medinger, and L. Forbes, "Buried-channel GaAs MESFETs with frequency-independent output conductance," *IEEE Elec. Device Lett.*, Vol. ED-L-8, pp. 88-89, March 1987.

(5) P. Ladbrook and S. Blight, "Low-field, low-frequency dispersion of transconductance in GaAs MESFETs with implication for other rate-dependent anomalies," *IEEE Trans. on Elec. Devices*, Vol. ED-35, pp. 257-267, March 1988.

(6) P.W. Van Der Walt, "Efficient technique for solving nonlinear mixer pumping problems," *Elec. Lett.*, Vol. 21, pp. 899-900, Sept. 1985.

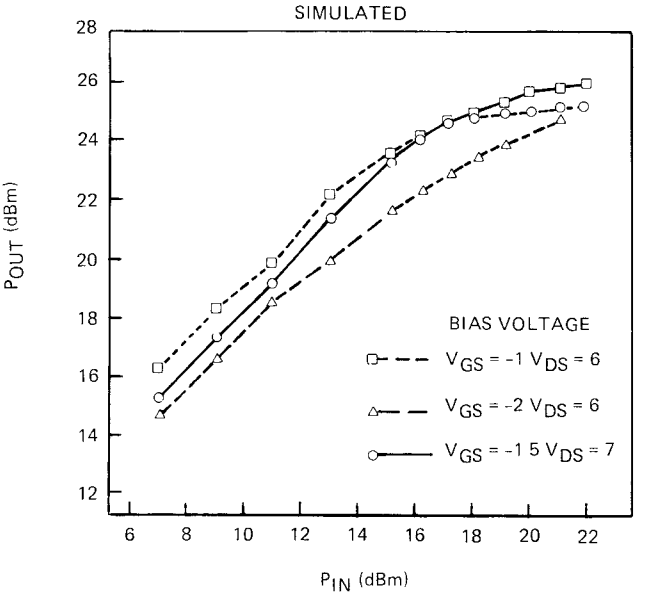

Figure 6 Simulated amplifier P_{out} versus P_{in} curves at 10.65 GHz.

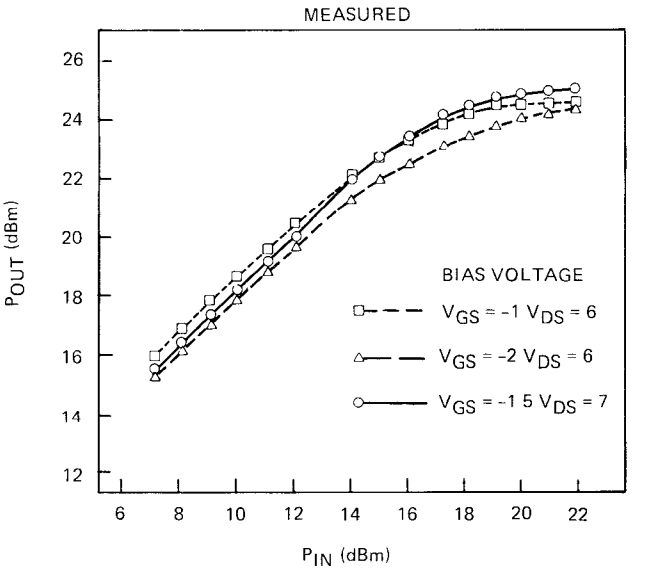

Figure 7 Measured amplifier P_{out} versus P_{in} curves at 10.65 GHz.

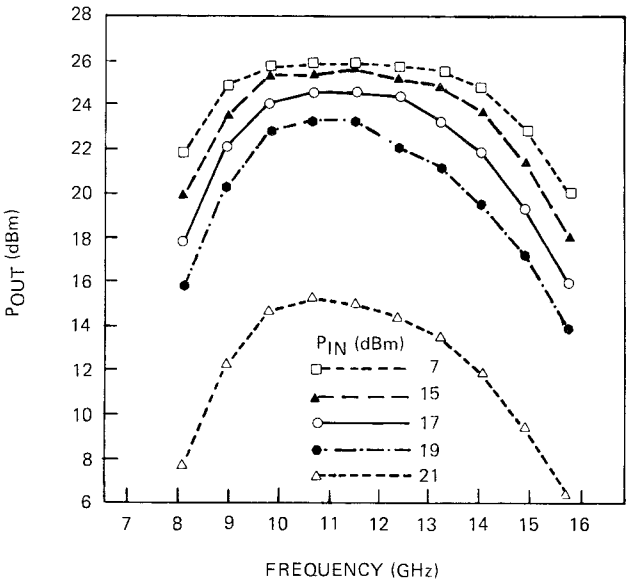

Figure 8 Simulated amplifier P_{out} versus frequency curves.

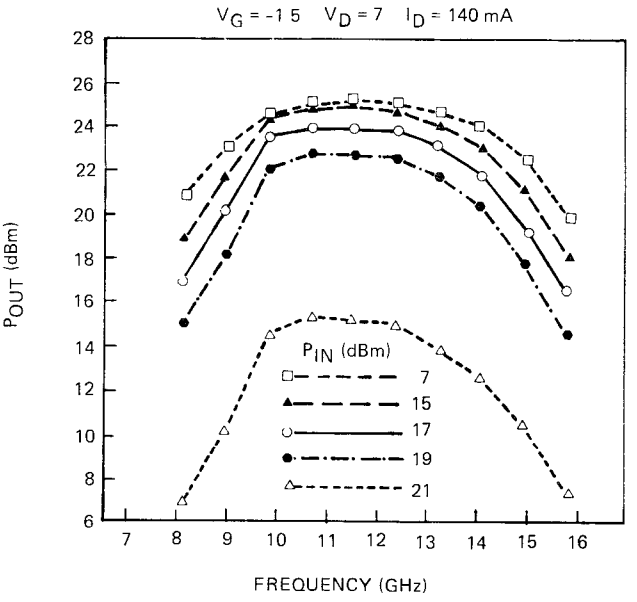

Figure 9 Measured amplifier P_{out} versus frequency curves.